

1
2 **40 Gb/s NRZ-DQPSK data wavelength conversion using four-wave mixing in a**
3 **quantum dash semiconductor optical amplifier**
4

5 Michael J. Connelly^a, Lukasz Krzczanowicz^a, Pascal Morel^b, Ammar Sharaiha^b,
6 Francois Lelarge^c, Romain Brenot^c, Siddharth Joshi^c and Sophie Barbet^c

7 ^aOptical Communications Research Group, Department of Electronic and Computer
8 Engineering, University of Limerick, Limerick, Ireland.

9 ^bLab-STICC, UMR CNRS 6285, École Nationale d'Ingénieurs de Brest CS 73862,
10 29238 Brest Cedex 3, France.

11 ^cAlcatel Thales III-V Laboratory, Route Departementale, 128, 91767 Palaiseau,
12 France.
13

14 **Abstract** – DQPSK modulation is attractive in high-speed optical communications
15 because of its resistance to fiber nonlinearities and its more efficient use of fiber
16 bandwidth compared to conventional intensity modulation schemes. Because of its
17 wavelength conversion ability and phase preservation, SOA four-wave mixing has
18 attracted much attention. We experimentally study the wavelength conversion of 40
19 Gbit/s (20 Gbaud) NRZ-DQPSK data using FWM in a Quantum Dash SOA with 20
20 dB gain and 5 dBm output saturation power. Q factor improvement and eye diagram
21 reshaping is shown for up to 3 nm pump-probe detuning and is superior to that
22 reported for a higher gain bulk SOA.

23
24 **Key words:** DQPSK, phase modulation, quantum-dash, semiconductor optical
25 amplifier, four-wave mixing, all optical wavelength conversion.
26

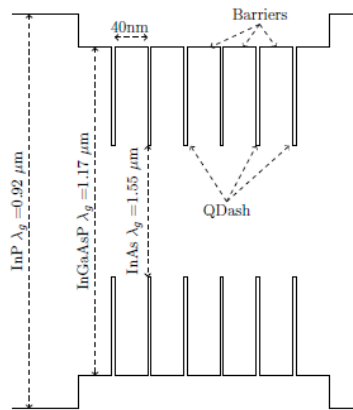
27 **1 Introduction**
28

29 The constantly increasing demand for data transmission rates leads to a need to
30 improve the effectiveness of bandwidth use. The Differential Quadrature Phase Shift
31 Keying (DQPSK) format has many advantages over conventional intensity
32 modulation schemes [1-4]. In particular it increases the spectral effectiveness by
33 transferring two bits per symbol and is relatively immune to fibre nonlinearities. In
34 order for the SOAs to be able to optimally work with the fast speed advanced
35 modulation formats, optimisation of the SOA structures are desired. An ideal SOA for
36 advanced modulation data should not only properly amplify signals, but also preserve
37 the phase relations between the symbols. For purely phase encoded signals a low
38 alpha-factor SOA is advantageous [5]. During the past few years, Quantum Dash
39 (QDash) devices have attracted considerable attention. Quantum dot and dash-based
40 SOAs are expected to have reduced noise figure and fast dynamic response compared
41 to quantum-well or bulk SOAs [6-7]. In this paper, we show FWM wavelength
42 conversion for 20 Gbaud (40 Gb/s) NRZ-DQPSK data using a QDash-SOA. Similar
43 work has been demonstrated for multiple quantum-well and bulk SOAs [8-10]. We
44 show significantly increased Q-factor and eye diagram reshaping, when compared to
45 the same operation conducted in a bulk SOA [10]. Wavelength conversion was
46 achieved for a positive detuning of up to 3 nm, with large Q factor improvements
47 obtainable for low quality probe input signals.
48

49 **2 SOA characteristics**

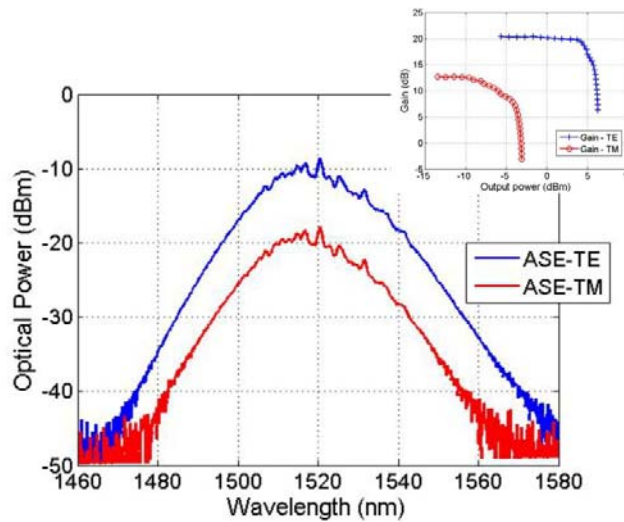
50

51 The SOA used is a custom packaged QDash device. The dashes are grown in a dash-
 52 in-a-barrier structure where the quantum dash emitting at $1.55 \mu\text{m}$ is buried in a
 53 quaternary barrier of $\lambda_g=1.17 \mu\text{m}$ [7]. The structure consists of six dash stack layers as
 54 shown in Fig 1. The SOA is processed using buried ridge stripe technology with a
 55 ridge width of $1.5 \mu\text{m}$. The waveguides are tilted at 7° and also feature a tilted mode
 56 shape convertor. The facets are treated with an anti-reflection coating. The SOA is
 57 operated at 500 mA bias current, with an unsaturated gain of approximately 20 dB at
 58 1530 nm, 5 dBm and 8dB saturation output power and polarization sensitivity
 59 respectively. The polarization dependent ASE spectrums and saturation characteristics
 60 are shown in Fig. 2.



61

62 Fig. 1. Dash-in-a-Barrier structure, showing 6 stack layers of InAs QDashes in
 63 InGaAsP barriers.
 64



65

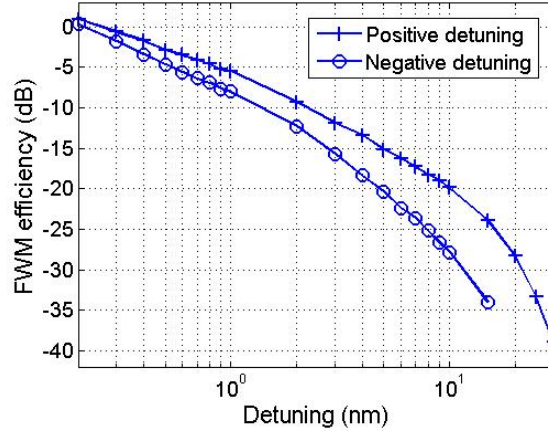
66

67 Fig. 2. Unsaturated ASE spectra and polarization dependent gain characteristics (at
 68 1530 nm) for a bias current of 500 mA. The spectral resolution is 1 nm.
 69

70

71 Fig. 3 shows the unmodulated FWM efficiency of the SOA for different detuning
 72 values. The FWM efficiency is defined as ratio of output conjugate power to the input
 73 probe power. The pump was a 1534 nm CW laser and its maximum power of -4 dBm.

74 For the purpose of wavelength conversion, it was desired to have the conjugate at the
 75 highest possible power level, which was obtained by adjusting the probe power for a
 76 detuning of 1nm. The maximum was achieved for a probe power of -7 dBm. The
 77 FWM efficiency was few dB lower than the one measured for a bulk SOA in our
 78 previous work [10].



79
80

81 Fig. 3. CW FWM efficiency versus detuning for input probe and pump powers of -7
 82 dBm, -4 dBm respectively.

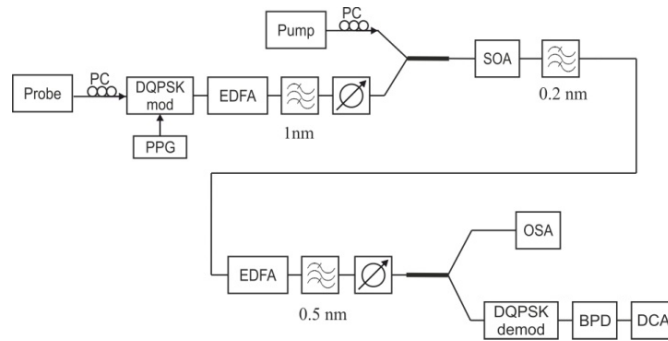
83

84 3 Experiment

85

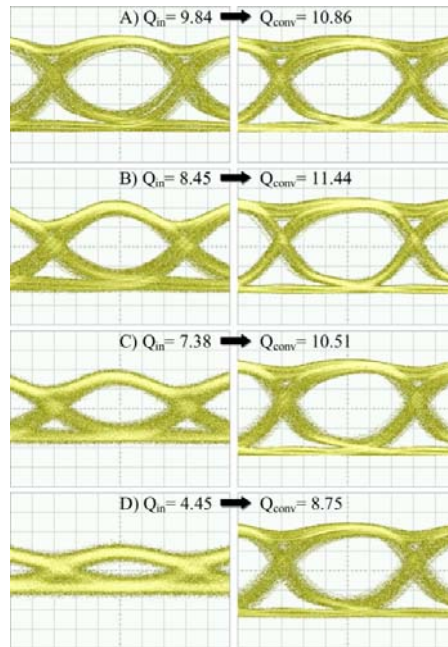
86 The DQPSK FWM experimental setup is shown in Fig. 4. The input pump power is -4
 87 dBm. The probe is a 20 Gbaud/s (40 Gb/s) NRZ-DQPSK 2^{15-1} pseudo random bit
 88 pattern. DQPSK modulation was carried out using a commercial modulator (Photline-
 89 MODBOX). The signal is amplified by an EDFA and its ASE reduced by a 1 nm
 90 filter. In order to separate the conjugate from the amplified pump and probe signals, a
 91 cascade of filters was used at the output of the SOA: a 0.2 nm FWHM fiber Bragg
 92 grating (FBG) centered at 1533 nm and a 0.5 nm tunable filter. The conjugate signal
 93 was then amplified by an EDFA and its ASE filtered out by a 0.5 nm filter. The
 94 DQPSK demodulator (Optoplex) consists of two delay-line interferometers that
 95 convert the I and Q components of the signal into intensity changes. The optical
 96 signals from the interferometer outputs are detected by balanced 23 GHz bandwidth
 97 photodiodes (Discovery Semiconductors Lab Buddy) and an 80 GHz electrical
 98 bandwidth Agilent 86100C digital communication analyzer. The demodulated I and Q
 99 components show almost identical performance. To this effect we concentrate on the I
 100 component for analysis purposes. The influence of probe power on the quality of the
 101 wavelength converted signal for a detuning of 1 nm was examined. The pump
 102 wavelength and power were set to 1534 nm and -4 dBm, respectively. The probe
 103 wavelength was set to 1535 nm. The input signal to the demodulator was fixed at -4.5
 104 dBm by adjusting the EFDA gain. The input and conjugate eye diagrams are shown in
 105 Fig. 5. The input Q factor increased with an increase in the probe power, whereas the
 106 wavelength converted signal Q-factor was highly dependent on the conjugate power,
 107 measured at the output of the SOA, reaching its maximum for a probe power of -10
 108 dBm as shown in Fig. 6.

109



110
111
112
113
114
115
116

Fig. 4. Experimental setup: PC (Polarization Controller), PPG (Pulse Pattern Generator), OSA (Optical Spectrum Analyzer), BPD (Balanced PhotoDetector), DCA Digital Communications Analyzer).



117
118
119
120
121
122

Fig. 5. Eye diagrams of input (left) and converted (right) signals for probe power of: A) -6 dBm, B) -10 dBm, C) -15 dBm, D) -20 dBm. The detuning is 1 nm. The horizontal scale is 8.3 ps/div.

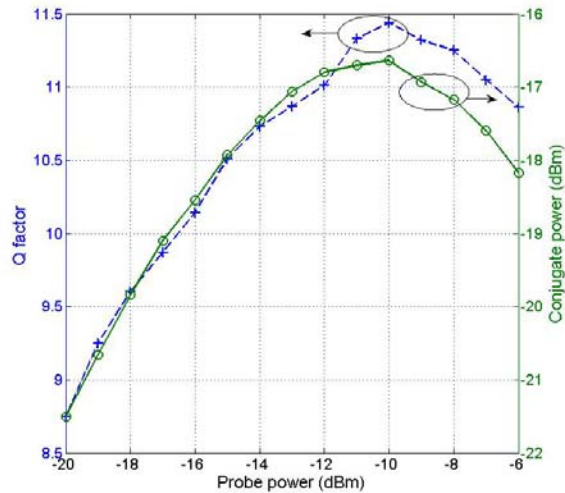
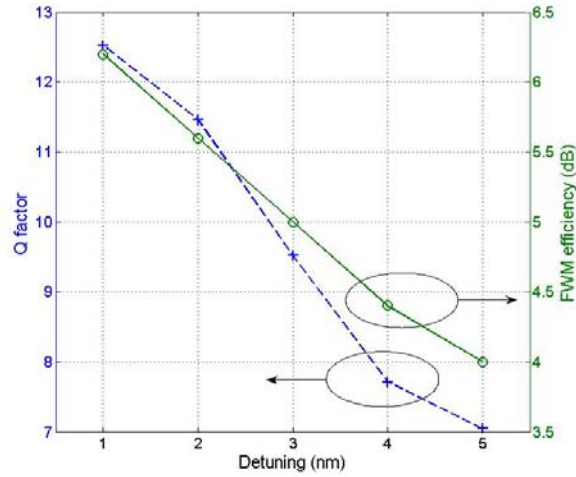


Fig. 6. Converted signal Q-factor and power for a detuning of 1nm.

In contrast to experimental results for a bulk SOA [10], where the converted eye diagram was degraded, large improvements in the converted signal were obtained for all investigated input probe powers, resulting in 2.63 dB improvement for the maximum converted Q-factor (from 8.45 to 11.44) for probe power of -10 dBm and a maximum improvement of 5.87 dB (from 4.45 to 8.75) for probe power of -20 dBm (the minimum investigated value). The quality of the converted signal for different detuning values was measured. Because of a non-tunable filter used, the pump and probe wavelengths were adjusted in order to maintain the conjugate signal at 1533.04 nm. The pump and probe powers were kept at -4 dBm and -10 dBm, respectively. The input Q factor was 8.45. The converted signal power was set to its maximum. The resulting Q-factor and FWM efficiency are shown in Fig. 7. As expected, the maximum obtainable Q-factor value decreases along with the conjugate power. For detuning up to 3 nm the Q-factor was improved, reaching a maximum value of 12.52 for 1 nm down-conversion. Fig. 8 shows a comparison of the eye diagrams for the input and converted signal for different detunings. A clear improvement in the eye diagram shape is seen for low detuning values.

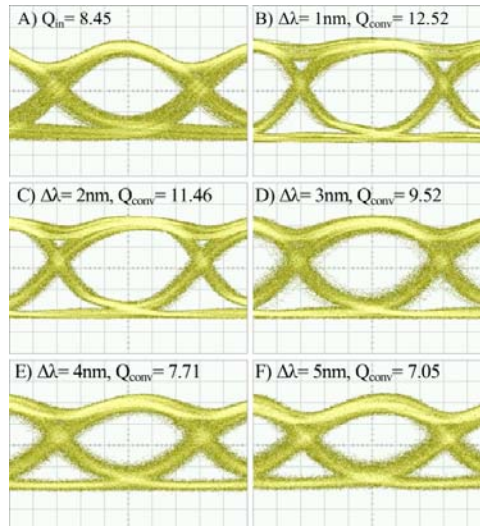
4 Conclusions

40 Gb/s NRZ-DQPSK FWM wavelength conversion in a QDash-SOA was demonstrated. Lossless wavelength conversion was achieved for positive detuning up to 3 nm, with significant improvements in the Q factor as well as eye diagram reshaping. The results are a noticeable improvement over similar experiments carried out using a bulk SOA. The physical reasons for such improvements are unclear but are probably linked to faster gain dynamics in QDash-SOAs compared to that in bulk SOAs. More theoretical work is required to determine the exact physical mechanisms leading to the FWM signal improvements.



157
158
159
160
161

Fig. 7. Converted signal Q-factor and FWM efficiency vs. detuning range.



162
163

Fig. 8. Eye diagrams for: (A) input probe and (B-F) wavelength converted signals for various positive detunings. The horizontal scale is 8.3 ps/div.

166
167
168

Acknowledgement

170

This research was supported by Science Foundation Ireland Investigator Grant 09/IN.1/I2641.

173

174

References

176

177 1. Gnauck A H, Winzer P J. Optical phase-shift-keyed transmission, Journal of
178 Lightwave Technology, 2005, 23(1):115- 130

179 2. Cho P S, Achiam Y, Levy-Yurista, Margalit M, Gross Y, Khurgin J B.

180 Investigation of SOA nonlinearities on the amplification of high spectral

181 efficiency signals. In Proceedings of Optical Fiber Communication Conference
182 OFC 2004, 1:211-212

183 3. Wang J, Kahn J M. Impact of chromatic and polarization-mode dispersions on
184 DPSK systems using interferometric demodulation and direct detection, Journal of
185 Lightwave Technology, 2004, 22(2):362-371

186 4. Ho K-P. Phase-modulated optical communication systems. Springer, 2005

187 5. Bonk R, Huber G, Vallaitis T, Koenig S, Schmogrow R, Hillerkuss D, Brenot R,
188 Lelarge F, Duan G H, Sygletos S, Koos C, Freude W, Leuthold J. Linear
189 semiconductor optical amplifiers for amplification of advanced modulation
190 formats, Optics Express, 2012, 20:9657-9672.

191 6. Akiyama T, Sugawara M, Arakawa Y. Quantum-dot semiconductor optical
192 amplifiers. Proceedings of the IEEE, 2007. 95(9):1757-1766

193 7. Lelarge F, Dagens B, Renaudier J, Brenot R, Accard A, van Dijk F, Make D, Le
194 Gouezigou O, Provost J, Poingt F, Landreau J, Drisse O, Derouin E, Rousseau B,
195 Pommereau F, Guang-Hua D. Recent advances on InAs/InP quantum dash based
196 semiconductor lasers and optical amplifiers operating at 1.55 μm ", IEEE Journal
197 of Selected Topics in Quantum Electronics, 2007, 13(1):111-124

198 Porzi C, Bogoni A, Contestabile G. Regeneration of DPSK signals in a saturated
199 SOA, IEEE Photonics Technology Letters, 2012, 24(18):1597–1599

200 8. Porzi C, Bogoni A, Contestabile G. Regenerative wavelength conversion of DPSK
201 signals through FWM in an SOA, IEEE Photonics Technology Letters, 2013,
202 25(2):175–178

203 9. Krzaczanowicz L, Connelly M J. 40 Gb/s NRZ-DQPSK data all-optical wavelength
204 conversion using four wave mixing in a bulk SOA", IEEE Photonics Technology
205 Letters, 2013, 25(24):2439,2441
206